J. Phys. B: At. Mol. Opt. Phys. 28 (1995) 3889–3899. Printed in the UK

Ionization in collisions of fast H^+ and He^{2+} ions with Fe and Cu atoms

C J Patton, M B Shah, M A Bolorizadeh†, J Geddes and H B Gilbody
Department of Pure and Applied Physics, The Queen's University of Belfast, Belfast, UK

Received 13 April 1995

Abstract. A crossed-beam technique, where the collision products have been selected by time-of-flight (TOF) spectroscopy with either a pulsed beam or coincidence counting, has been used to study pure ionization of Fe and Cu by 70–1440 keV amu^{-1} H^+ and 35–425 keV amu^{-1} He^{2+} ions. Cross sections for the formation of q times ionized Fe and Cu products by pure ionization have been determined for $q = 1$–4. A comparison with the corresponding (previously measured) cross sections for transfer ionization shows that, in the energy range considered, Fe^+ and Cu^+ ions arise predominantly through pure ionization. However, for $q \geqslant 2$, contributions from both transfer ionization and pure ionization are important. Pure ionization becomes dominant at energies which increase as q increases. Measured cross sections for pure ionization have been successfully fitted to values based on an independent electron model approximation.

1. Introduction

In recent work in this laboratory (Patton *et al* 1994, Shah *et al* 1995a) we have used a crossed-beam coincidence counting technique to study (for the first time) electron capture and transfer ionization in collisions of H^+ and He^{2+} ions with Fe and Cu atoms within the range 35–1440 keV amu^{-1}. For H^+ impact, cross sections ${}_{10}\sigma_{0q}$ for one-electron capture processes

$$H^+ + X \rightarrow H + X^{q+} + (q-1)e \tag{1}$$

for $q = 1$–4 for Fe and $q = 1$–5 for Cu have been determined. Here, $q = 1$ corresponds to simple charge transfer while $q > 1$ corresponds to transfer ionization, where electron capture is accompanied by multiple ionization of the target. In the case of He^{2+} impact, corresponding cross sections ${}_{20}\sigma_{1q}$ for one-electron capture and ${}_{20}\sigma_{0q}$ for two-electron capture, leading to product ions of specified q, were determined for values of q up to seven. These measurements, which were considered in terms of a model involving electron capture from particular subshells, provided a useful insight into the mechanisms of multiple ionization of heavy metallic species by ion impact. There is interest in the collisional formation of both Fe and Cu in all stages of ionization in the astrophysical context and in controlled thermonuclear fusion research.

In the present work we have extended our previous measurements on Fe and Cu to include studies of the pure (or direct) ionization corresponding to the processes

$$H^+ + X \rightarrow H^+ + X^{q+} + qe \tag{2}$$

† Permanent address: Department of Physics, Shahid Bahonar University, Kerman, Iran.

0953-4075/95/173889+11$19.50

and

$$He^{2+} + X \rightarrow He^{2+} + X^{q+} + qe \tag{3}$$

for the first time. Cross sections ${}_{10}\sigma_{1q}$ and ${}_{20}\sigma_{2q}$ for (2) and (3) have been determined for $q = 1$–4 within the range 70–1440 keV amu^{-1} for H^+ impact, and for $q = 1$–3 within the range 35–425 keV amu^{-1} for He^{2+} impact. The present cross sections for pure ionization have been considered in relation to the corresponding cross sections for one-electron capture leading to the same charge states q measured previously (Patton *et al* 1994, Shah *et al* 1995a). An independent electron model approximation has also been invoked to successfully describe our measured cross sections for pure ionization in terms of electron removal from the outer subshells.

2. Experimental approach

2.1. General description

The present experimental arrangement has evolved from previous work in this laboratory originally concerned with studies of the ionization of atomic hydrogen (Shah and Gilbody 1981), but subsequently extended to a variety of stable targets including metallic atoms (cf Shah *et al* 1992). Since details of the general approach and measurement procedure have been given previously, only an outline need be presented here.

An energy and momentum analysed beam of H^+ or He^{2+} ions was arranged to intersect (at right angles) a thermal energy beam of either Fe or Cu atoms in a high-vacuum region maintained at about 6×10^{-8} Torr. The latter were derived from a specially developed oven source which has been described previously (McCallion *et al* 1992).

Slow Fe^{q+} or Cu^{q+} product ions and electrons were extracted from the crossed-beam region by a transverse electric field applied between two high-transparency grids which was high enough to ensure essentially complete collection. The slow ions and electrons were separately counted by two particle multipliers. Over most of the energy range, product ions of particular charge states q were selectively distinguished and separated from background gas ion collision products by time-of-flight analysis, using a pulsed beam technique together with a delayed extraction pulse (Shah *et al* 1987). At the higher energies the two particle multipliers were used in a coincidence arrangement in which selected X^{q+} products were counted in coincidence with the electrons from the same events. Figure 1 shows a typical time-of-flight spectrum corresponding to Cu^{q+} formation for $q = 1$–4 for collisions of a pulsed beam of 62 keV amu^{-1} He^{2+} ions with Cu.

2.2. Measuring, calibration and normalization procedure

The calibration and normalization procedure was similar to that described in previous work (cf Shah *et al* 1992). The primary ion beam was pulsed at a frequency of 100 kHz with a pulse duration of 200 ns. Slow ion products were extracted by means of a pulsed transverse field and identified by TOF spectroscopy. The slow ion yield $S_i(X^{q+})$ per unit primary ion current could then be related to a cross section $\sigma_q(i)$ for X^{q+} formation by ion impact through the expression

$$\sigma_q(i) = S_i(X^{q+})/k(X^{q+})\mu \tag{4}$$

where $k(X^{q+})$ is the efficiency of detection of X^{q+} ions and μ is the X atom target thickness traversed by the primary beam. By means of a sliding mount, a pulsed beam of electrons (with the same pulse duration and repetition rate as the ion beam) was substituted for the

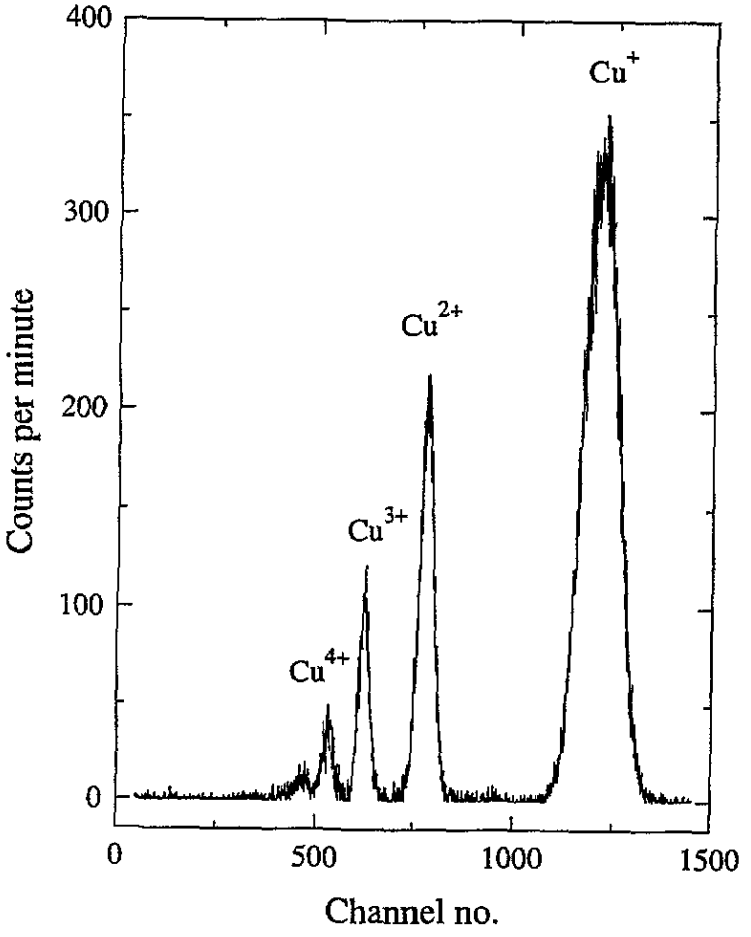

Figure 1. The time-of-flight Cu^{q+} product ion spectrum for collisions of a pulsed beam of 62 keV amu^{-1} He^{2+} ions with Cu. The adjacent channel separation is 2 ns.

ion beam in precisely the same position, with the target conditions unchanged. In this case, the yield $S_e(X^{q+})$ of X^{q+} ions per unit electron current is related to a cross section $\sigma_q(e)$ for electron-impact ionization through the expression

$$\sigma_q(e) = S_e(X^{q+})/k(X^{q+})\mu. \tag{5}$$

It was then possible to determine $\sigma_q(i)$ in (4) using values of $k(X^{q+})\mu$ from (5) where values of $\sigma_q(e)$ are known from our previous measurements (Shah *et al* 1993, Bolorizadeh *et al* 1994) which in turn were normalized to absolute values measured by Freund *et al* (1990).

Cross sections for pure ionization could then be determined from our normalized values of $\sigma_q(i)$. Cross sections ${}_{10}\sigma_{1q}$ for $q = 1$–3 were obtained from the difference ${}_{10}\sigma_{1q} = (\sigma_q(i) - {}_{10}\sigma_{0q})$ using our previously measured transfer-ionization cross sections ${}_{10}\sigma_{0q}$. In the same way for He^{2+} impact, cross sections ${}_{20}\sigma_{21} = (\sigma_1(i) - {}_{20}\sigma_{11})$ for single ionization were obtained while cross sections ${}_{20}\sigma_{2q}$ for multiple ionization were derived from cross sections $\sigma_q(i)$ by subtracting our previously measured values of ${}_{20}\sigma_{1q}$ and ${}_{20}\sigma_{0q}$ for transfer ionization involving both one- and two-electron capture.

Practical difficulties associated with our electronic circuitry used to pulse the ion beam precluded measurements above 1 MeV amu^{-1} for H^+ ions and 360 keV amu^{-1} for He^{2+} ions. At these higher energies where contributions from transfer ionization can be assumed to be negligibly small, measurements of the slow X^{q+}–electron coincidence signals allow an apparent ionization cross section $\sigma_q^i(X^{q+})$ for the formation of X^{q+} ions to be determined from the equation

$$\sigma_q^i(X^{q+}) = S_q / k(X^{q+}) k(qe) \mu \tag{6}$$

where $k(qe)$ is the efficiency of detection of a group of q electrons. In order to determine the product $k(X^{q+})k(qe)\mu$ in equation (6), we relied on our high-energy values of $\sigma_q(i)$ where the transfer-ionization contribution is negligible. Cross sections ${}_{10}\sigma_{14}$ for H^+ impact at higher energies were obtained using the coincidence technique, where values of the product $k(X^{4+})k(4e)$ were estimated on the basis of probability arguments from those determined for $q = 1$–3.

Measurements of ${}_{10}\sigma_{1q}$ for $q = 1$–4 were carried out for 70–1440 keV amu^{-1} H^+ ions in Fe and 80–1440 H^+ ions in Cu. Measurements of ${}_{10}\sigma_{1q}$ for $q = 1$–3 were carried out for 35–360 keV amu^{-1} He^{2+} ions in Fe and 35–425 keV amu^{-1} He^{2+} ions in Cu.

3. Results and discussion

Our measured cross sections ${}_{10}\sigma_{1q}$ and ${}_{20}\sigma_{2q}$ for the pure ionization of Fe and Cu by H^+ and He^{2+} ions are given in tables 1–4. The indicated uncertainties (at the 67% confidence level) reflect the degree of reproducibility of the individual cross sections. All the cross sections shown are subject to an additional estimated uncertainty of ±12% arising from our normalization procedure.

Table 1. Cross sections ${}_{10}\sigma_{1q}$ for the pure ionization of Fe by H^+ ions leading to Fe^{q+} product ions for $q = 1$–4.

Energy (keV amu^{-1})	${}_{10}\sigma_{11}$ (10^{-16} cm^2)	${}_{10}\sigma_{12}$ (10^{-17} cm^2)	${}_{10}\sigma_{13}$ (10^{-18} cm^2)	${}_{10}\sigma_{14}$ (10^{-19} cm^2)
70	7.5 ± 0.4	—	—	—
80	7.2 ± 0.3	—	—	—
93	6.8 ± 0.4	5.6 ± 1.0	—	—
108	6.0 ± 0.3	4.8 ± 0.7	—	—
125	5.5 ± 0.4	5.0 ± 0.6	—	—
150	4.60 ± 0.28	4.5 ± 0.4	—	—
175	3.98 ± 0.25	4.8 ± 0.3	4.5 ± 1.5	—
210	3.34 ± 0.22	3.5 ± 0.4	3.8 ± 1.1	—
250	2.87 ± 0.17	3.4 ± 0.3	3.3 ± 1.0	—
300	2.59 ± 0.14	3.2 ± 0.3	5.8 ± 1.2	—
355	2.19 ± 0.10	2.5 ± 0.3	4.6 ± 1.0	—
420	2.00 ± 0.14	2.5 ± 0.2	5.4 ± 1.0	—
500	1.69 ± 0.10	2.2 ± 0.2	4.3 ± 0.7	7.5 ± 1.7
600	1.42 ± 0.07	1.92 ± 0.16	4.6 ± 0.6	8.3 ± 1.7
720	1.27 ± 0.05	1.81 ± 0.12	3.6 ± 0.4	8.3 ± 1.7
850	1.17 ± 0.05	1.60 ± 0.15	3.6 ± 0.3	6.8 ± 1.3
1000	0.98 ± 0.05	1.38 ± 0.12	3.3 ± 0.3	5.7 ± 1.0
1200	0.85 ± 0.06	1.24 ± 0.12	2.6 ± 0.3	5.3 ± 0.9
1440	0.71 ± 0.05	1.06 ± 0.10	2.2 ± 0.3	4.3 ± 0.5

Table 2. Cross sections $_{20}\sigma_{2q}$ for the pure ionization of Fe by He^{2+} ions leading to Fe^{q+} product ions for $q = 1$–3.

Energy (keV amu^{-1})	$_{20}\sigma_{21}$ (10^{-16} cm^2)	$_{20}\sigma_{22}$ (10^{-16} cm^2)	$_{20}\sigma_{23}$ (10^{-17} cm^2)
35	21.2 ± 0.8	—	—
40	23.1 ± 1.0	—	—
47	22.5 ± 0.8	1.7 ± 0.4	—
54	22.1 ± 0.9	1.6 ± 0.3	—
62	20.3 ± 0.9	1.3 ± 0.2	—
75	18.6 ± 0.9	1.4 ± 0.2	—
88	16.8 ± 0.8	1.3 ± 0.2	—
105	15.1 ± 0.6	1.2 ± 0.2	—
125	13.4 ± 0.5	1.24 ± 0.16	—
150	12.3 ± 0.5	1.26 ± 0.09	—
180	11.3 ± 0.5	1.27 ± 0.09	2.1 ± 0.8
213	9.5 ± 0.4	1.10 ± 0.08	2.3 ± 0.8
250	8.7 ± 0.4	1.12 ± 0.07	2.7 ± 0.5
300	7.7 ± 0.3	1.02 ± 0.10	3.1 ± 0.5
360	6.7 ± 0.3	0.82 ± 0.10	3.0 ± 0.5

Table 3. Cross sections $_{10}\sigma_{1q}$ for the pure ionization of Cu by H^+ ions leading to Cu^{q+} product ions for $q = 1$–4.

Energy (keV amu^{-1})	$_{10}\sigma_{11}$ (10^{-16} cm^2)	$_{10}\sigma_{12}$ (10^{-17} cm^2)	$_{10}\sigma_{13}$ (10^{-18} cm^2)	$_{10}\sigma_{14}$ (10^{-19} cm^2)
80	5.5 ± 0.5	—	—	—
93	4.8 ± 0.4	—	—	—
108	4.4 ± 0.4	—	—	—
125	4.15 ± 0.28	2.3 ± 0.3	—	—
150	3.88 ± 0.26	2.4 ± 0.2	—	—
175	3.54 ± 0.22	2.4 ± 0.2	—	—
210	3.14 ± 0.20	2.4 ± 0.2	—	—
250	2.65 ± 0.13	2.3 ± 0.2	5.1 ± 1.0	—
300	2.30 ± 0.10	2.3 ± 0.18	5.7 ± 0.6	—
360	2.05 ± 0.10	1.90 ± 0.14	5.2 ± 0.5	—
425	1.85 ± 0.08	1.96 ± 0.14	4.8 ± 0.5	—
500	1.70 ± 0.06	1.88 ± 0.18	5.2 ± 0.5	6.0 ± 3.0
600	1.48 ± 0.07	1.65 ± 0.11	4.1 ± 0.4	7.0 ± 2.0
720	1.35 ± 0.07	1.43 ± 0.08	3.4 ± 0.3	7.0 ± 2.0
850	1.13 ± 0.06	1.21 ± 0.09	3.5 ± 0.3	5.0 ± 1.2
1000	0.97 ± 0.06	1.09 ± 0.09	2.7 ± 0.2	5.2 ± 1.0
1200	1.01 ± 0.06	1.06 ± 0.10	2.6 ± 0.3	3.5 ± 0.9
1440	0.83 ± 0.06	0.86 ± 0.09	2.1 ± 0.3	3.8 ± 0.7

3.1. General discussion

In figure 2, measured cross sections $_{10}\sigma_{1q}$ and $_{20}\sigma_{2q}$ for pure ionization of Fe and Cu by H^+ and He^{2+} ions may be compared with the corresponding one-electron capture cross sections $_{10}\sigma_{0q}$ and $_{20}\sigma_{1q}$ measured previously (Patton *et al* 1994, Shah *et al* 1995a). Equivelocity pure ionization cross sections can be seen to decrease rapidly with increasing q. Singly-charged ion production can be seen to be dominated by pure ionization over the energy range

Table 4. Cross sections $_{20}\sigma_{2q}$ for the pure ionization of Cu by He^{2+} ions leading to Cu^{q+} product ions for $q = 1$–3.

Energy (keV amu^{-1})	$_{20}\sigma_{21}$ (10^{-16} cm^2)	$_{20}\sigma_{22}$ (10^{-16} cm^2)	$_{20}\sigma_{23}$ (10^{-17} cm^2)
35	22.7 ± 1.5	—	—
40	24.0 ± 2.0	—	—
47	20.1 ± 1.2	—	—
54	21.5 ± 1.5	1.1 ± 0.4	—
62	18.5 ± 1.0	0.9 ± 0.3	—
75	15.8 ± 1.2	1.3 ± 0.2	3.2 ± 1.3
88	15.0 ± 1.3	1.3 ± 0.2	3.3 ± 1.0
105	13.7 ± 1.0	1.2 ± 0.2	2.0 ± 1.0
125	11.5 ± 0.7	1.2 ± 0.1	3.2 ± 0.8
150	9.8 ± 0.6	1.0 ± 0.1	2.5 ± 0.6
180	10.3 ± 0.5	1.2 ± 0.1	4.3 ± 0.6
213	8.5 ± 0.4	1.04 ± 0.09	3.2 ± 0.5
250	8.2 ± 0.4	0.95 ± 0.07	3.6 ± 0.5
300	7.2 ± 0.3	0.98 ± 0.07	3.5 ± 0.5
360	6.9 ● 0.3	1.00 ± 0.08	3.3 ± 0.5
425	6.2 ± 0.4	—	—

considered, but for $q \geqslant 2$, transfer ionization provides an increasingly important contribution to slow ion formation as the impact energy decreases. Pure ionization cross sections $_{10}\sigma_{1q}$ and $_{20}\sigma_{2q}$ can be seen to begin to exceed the corresponding electron-capture cross sections at energies which increase progressively with q. The pure ionization cross sections can be seen to decrease much more slowly with increasing velocity than the corresponding high-velocity cross sections for transfer ionization.

In figure 3, the present cross sections for pure ionization by H^+ and He^{2+} ions may be compared with the cross sections predicted by McGuire (1977a, b) on the basis of the first Born approximation and the Z^2 scaling relation, where Z is the atomic number of the projectile. The predicted contributions to single ionization from the 4s and 3d subshells, which are shown separately, indicate that while the 4s subshell contribution is dominant at our lower energies, the 3d contribution is dominant at the highest energies considered. Cross sections are divided by Z^2 to facilitate comparison.

Our cross sections for single ionization by H^+ and He^{2+} impact scaled in this way can be seen to exhibit the expected tendency to converge to a common value at high velocities which, in the case of Fe, is quite well described by the Born calculations. In the case of Cu, the calculations appear to overestimate the 3d contribution. For $q = 2$, it is also interesting and rather surprising to note a tendency of the scaled cross sections to converge at high velocities. This trend cannot be clearly discerned in the available data for $q = 3$.

3.2. Independent electron model description of ionization

In our previous studies of transfer ionization in iron and copper (Shah *et al* 1995a, b) we have successfully described our observed q-state distribution in terms of a model based on an independent electron description of multiple ionization (cf McGuire 1991). It is interesting to try to describe the present results for pure ionization using a similar approach. In this case, we assume that the probability P for the removal of an electron from a particular

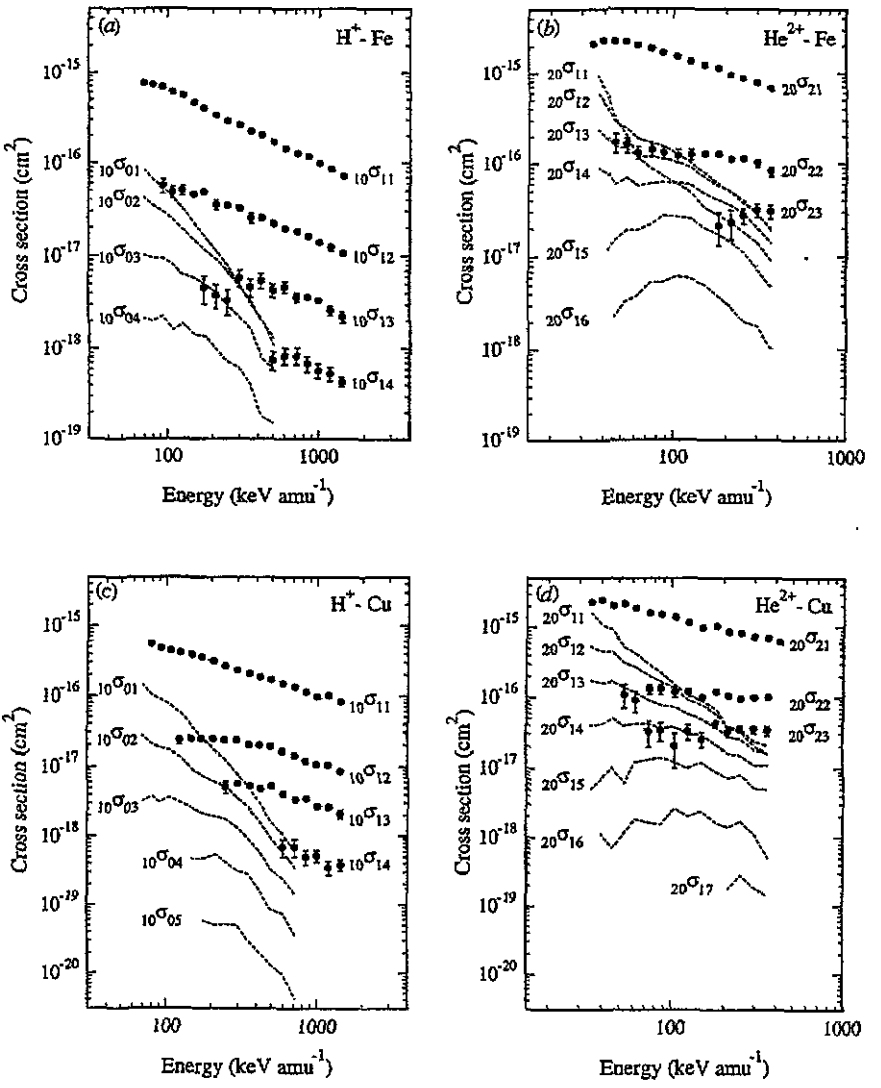

Figure 2. Present cross sections for pure ionization (●) compared with corresponding cross sections for one-electron capture (– – –) measured previously by Patton *et al* (1994) and Shah *et al* (1995a): (*a*) cross sections $_{10}\sigma_{1q}$ and $_{10}\sigma_{0q}$ for H^+–Fe collisions; (*b*) cross sections $_{20}\sigma_{2q}$ and $_{20}\sigma_{1q}$ for He^{2+}–Fe collisions; (*c*) cross sections $_{10}\sigma_{1q}$ and $_{10}\sigma_{0q}$ for H^+–Cu collisions; and (*d*) cross sections $_{20}\sigma_{2q}$ and $_{20}\sigma_{1q}$ for He^{2+}–Cu collisions.

subshell in the target, in the process of ionization, can be approximated by the expression

$$P(b) = P(0)\exp(-b/R) \tag{7}$$

where b is the impact parameter and $P(0)$ and R are constants for a given subshell. An expression of this form, which has recently been successfully used by Matsuo *et al* (1994) to describe pure ionization, also seems to be in good accord with the formulation suggested by McGuire and Richard (1973) for velocities in the present range.

As in our previous description of transfer ionization, we assume that pure ionization of Fe and Cu primarily involves electron removal from the 4s and 3d subshells. We have

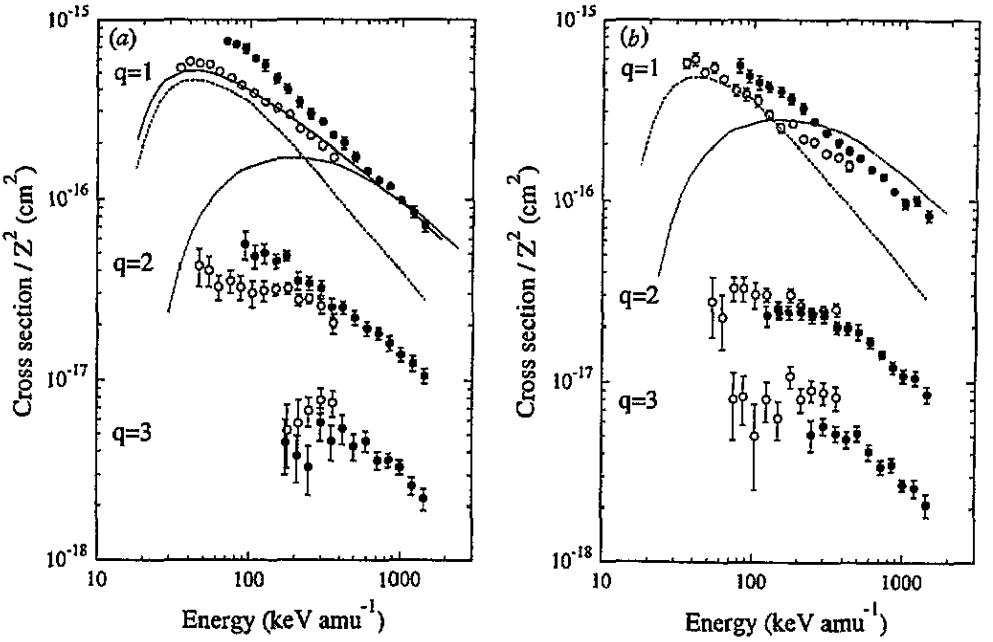

Figure 3. Cross sections/Z^2 for pure ionization of Fe in (*a*) and pure ionization of Cu in (*b*) by H^+ ions (●) and by He^{2+} ions (○). Theoretical predictions based on the first Born approximation by McGuire (1977a,b) are shown as follows: (——), cross section for single ionization; (– – –), cross section for removal of a 4s electron; and (·····), cross section for removal of a 3d electron.

previously demonstrated that the probability of electron removal from these subshells is roughly equal in the one-electron capture process so that, in this case, we assume that the individual probabilities $P(0)$ are the same for each subshell. Cross sections for pure ionization resulting in the removal of q electrons from a total of N may then be described by the expression

$$_{10}\sigma_{1q} \text{ or } _{20}\sigma_{2q} = 2\pi \int_0^\infty \binom{N}{q} P(b)^q (1 - P(b))^{(N-q)} b \, db \tag{8}$$

where $\binom{N}{q}$ is the binomial coefficient.

Values of $_{10}\sigma_{1q}$ and $_{20}\sigma_{2q}$ predicted by equation (8) have been fitted to our experimentally measured values using a weighted least-squares fit. The results of these fits are shown in figure 4, while the values of $P(0)$ and R derived from the fitting procedure are shown in figure 5. It is noted that R is more strongly dependent on projectile charges than $P(0)$. The fits to the pure ionization data for $q = 1$–4 can be seen to be generally very satisfactory. At energies where there are no experimental data for higher q states, we have used the values of $P(0)$ and R to predict the magnitude of the cross section.

4. Conclusions

The present studies of pure ionization of Fe and Cu by H^+ and He^{2+} impact, leading to product charge states q up to 4, provide an interesting comparison with our previous

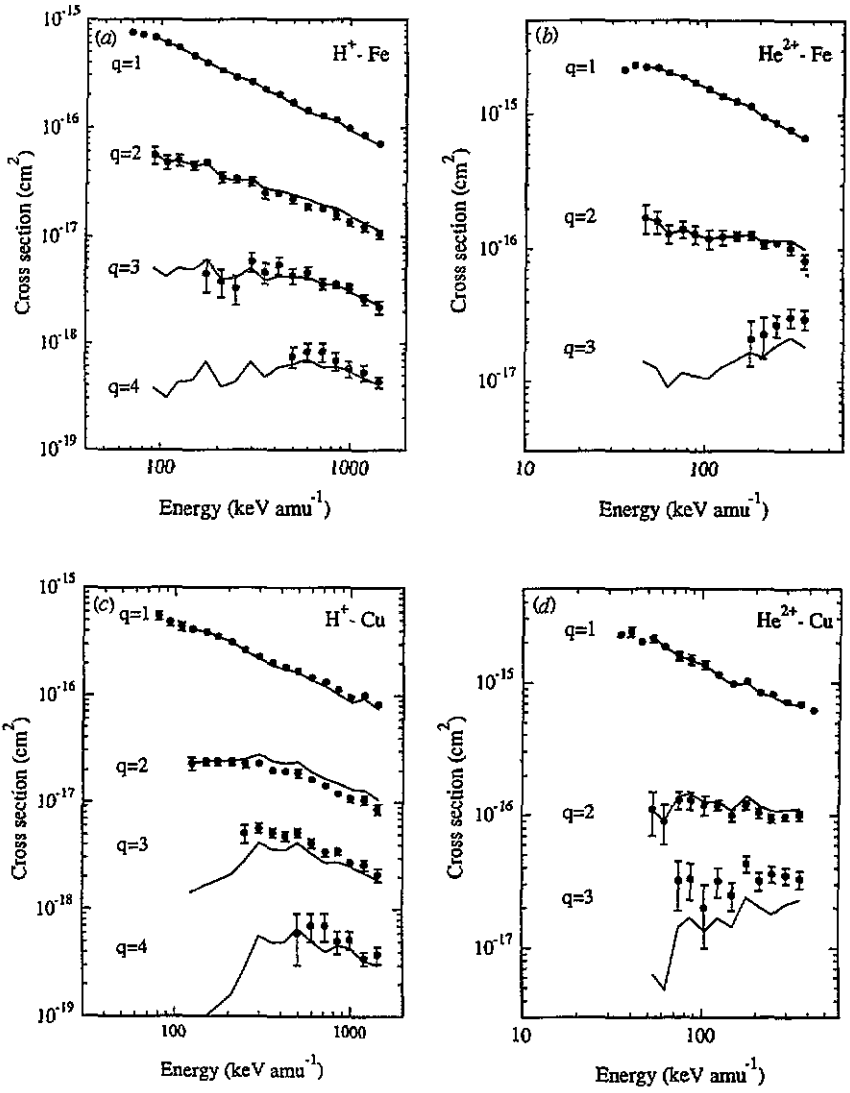

Figure 4. Present cross sections $_{10}\sigma_{1q}$ and $_{20}\sigma_{2q}$ for pure ionization (●) compared with fits (——) based on an independent electron model of ionization (see text): (*a*) H^+–Fe collisions; (*b*) He^{2+}–Fe collisions; (*c*) H^+–Cu collisions; and (*d*) He^{2+}–Cu collisions.

measurements of electron capture. The relative importance of pure ionization and electron-capture processes leading to the formation of singly- and multiply-charged product ions has been clearly established for 70–1440 keV amu^{-1} H^+ ions and 35–425 keV amu^{-1} He^{2+} ions. Measured cross sections for single ionization are shown to be in reasonable general accord with predictions based on the first Born approximation, in which electron removal from the 4s and 3d subshells is considered. As in previous studies of electron capture, we have used an independent electron model to satisfactorily describe our observed cross sections for $q = 1$–4 formation.

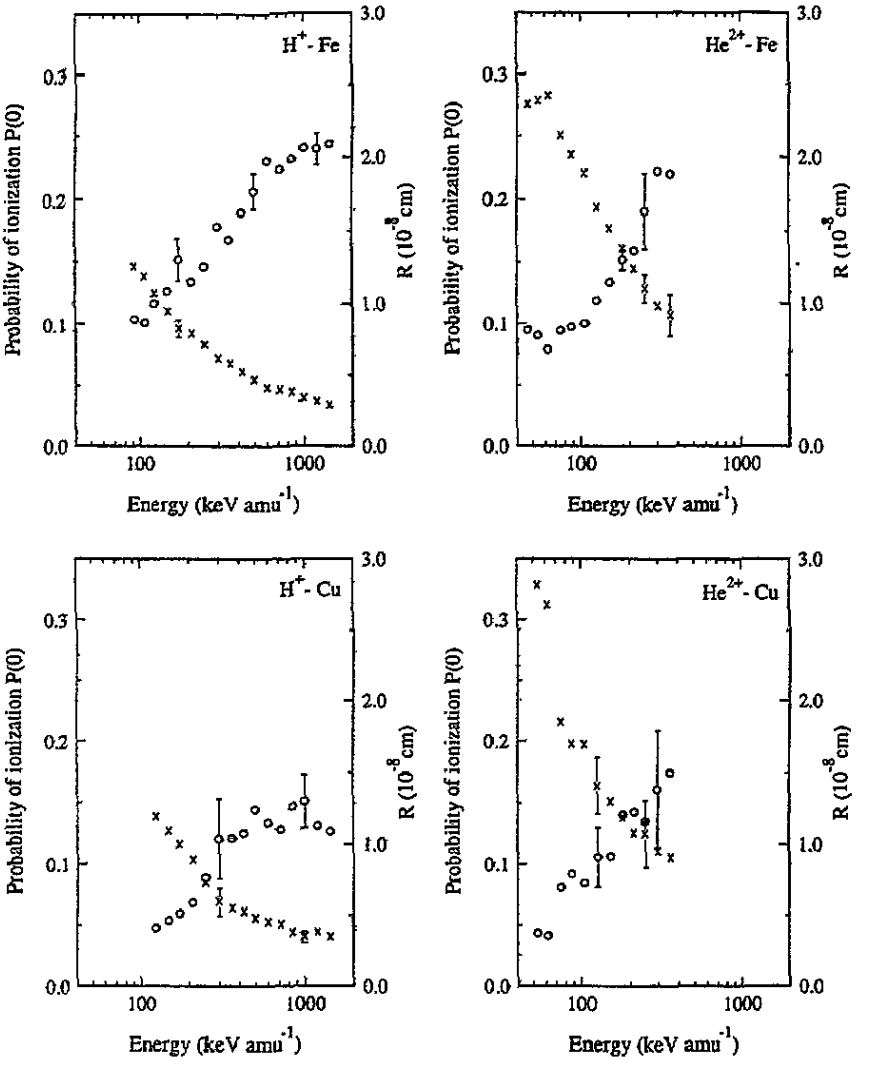

Figure 5. Plots showing the energy dependence of the fitting parameters $P(0)$ (○) and R (×) in the expression for the ionization probability $P(b) = P(0)\exp(-b/R)$. A few representative limits of uncertainty are shown.

Acknowledgments

This research forms part of a programme supported by a rolling research grant from the Engineering and Physical Sciences Research Council. One of us (CJP) is also indebted to the Department of Education, Northern Ireland for the award of a Research Studentship.

References

Bolorizadeh M A, Patton C J, Shah M B and Gilbody H B 1994 *J. Phys. B: At. Mol. Opt. Phys.* **27** 175
Freund R S, Wetsel R C, Shul R J and Hayes T R 1990 *Phys. Rev.* A **41** 3575
Matsuo T, Tonuma T, Kumagai H and Tawara H H 1994 *Phys. Rev.* A **50** 1178

McCallion P, Shah M B and Gilbody H B 1992 *J. Phys. B: At. Mol. Opt. Phys.* **25** 1051
McGuire E J 1977a *Phys. Rev.* A **16** 62
——1977b *Phys. Rev.* A **16** 73
McGuire J H 1991 *Advances in Atomic Molecular Optical Physics* vol 29, ed D R Bates and B Bederson (New York: Academic) p 217
McGuire J H and Richard P 1973 *Phys. Rev.* A **8** 1374
Patton C J, Bolorizadeh M A, Shah M B, Geddes J and Gilbody H B 1994 *J. Phys. B: At. Mol. Opt. Phys.* **27** 3695
Shah M B and Gilbody H B 1981 *J. Phys. B: At. Mol. Phys.* **14** 2361
Shah M B, Elliott D S and Gilbody H B 1987 *J. Phys. B: At. Mol. Phys.* **20** 3501
Shah M B, McCallion P, Itoh Y and Gilbody H B 1992 *J. Phys. B: At. Mol. Opt. Phys.* **25** 3693
Shah M B, McCallion P, Okuno K and Gilbody H B 1993 *J. Phys. B: At. Mol. Opt. Phys.* **26** 2393
Shah M B, Patton C J, Bolorizadeh M A, Geddes J and Gilbody H B 1995a *J. Phys. B: At. Mol. Opt. Phys.* **28** 1821
Shah M B, Patton C J, Geddes J and Gilbody H B 1995b *Nucl. Instrum. Methods Phys. Res.* B **98** 280